UDC 539.4

Theoretical and Experimental Evaluation of Performance of a CNG Engine and the Pistons Fatigue Lives Employing Modified Fatigue Criteria

M. Shariyat[1], S. A. Jazayeri, and J. Fathi Sola

Toosi University of Technology, Tehran, Iran

[1] m_shariyat@yahoo.com; shariyat@kntu.ac.ir

УДК 539.4

Теоретическая и экспериментальная оценка рабочих характеристик газового двигателя внутреннего сгорания и параметров усталостной долговечности его поршней с помощью модифицированных усталостных критериев

М. Шарият, С. А. Джазаери, Дж. Фатхи Сола

Технологический университет им. К. Н. Туси, Тегеран, Иран

Представлена систематизированная методика теоретической оценки рабочих характеристик газового двигателя внутреннего сгорания и параметров усталостного разрушения его поршней и выполнена ее экспериментальная верификация путем натурных испытаний двигателя. Методика включает в себя моделирование процессов внутреннего сгорания и теплопередачи, кинематический и динамический анализы движущихся частей двигателя, анализ переходного термоупругого процесса и усталостного разрушения при комплексном термомеханическом нагружении. Расчетные значения давления и температуры для различных углов поворота кривошипно-шатунного механизма хорошо согласуются с экспериментальными данными. Результаты расчета характеристик теплопередачи подтверждаются данными экспериментальных измерений с помощью термодатчиков Temglugs. Движущаяся система считается не дискретной, а непрерывной с точно моделируемыми нелинейными многоточечными контактными реакциями. При расчетах усталостной долговечности используются модифицированные критерии Мак-Диармида и Финдли для многоцикловой усталости, предложенные одним из авторов этой работы. Выполнена их верификация с помощью экспериментальных данных. Методика может использоваться для оценки целесообразности преобразования бензинового двигателя в газовый. Расчетные данные о различных усталостных характеристиках, полученные при термомеханическом нагружении, подтверждают точность предложенных критериев усталости и показывают, что срок службы поршня двигателя внутреннего сгорания существенно уменьшается, если вместо бензина используется природный газ.

Ключевые слова: моделирование внутреннего сгорания, динамический анализ, двигатель, поршень, усталостное разрушение, эксперимент.

Introduction. Due to fuel and pollution crises encountered in the two past decades and serious worries about the future of the petroleum resources, remarkable researches recently have been performed to replace the gasoline by more reliable or more economic fuels. In some countries, researchers have proposed using the natural gas, e.g., in the form of compressed natural gas (CNG), as an alternative

© M. SHARIYAT, S. A. JAZAYERI, J. FATHI SOLA, 2012

fuel. Due to different combustion characteristics, employing different fuels in the gasoline-based engines leads to some side effects such as performance degradation, increases in the thermal losses, emission, and lower fatigue lives for the components. Therefore, predicting the consequences is a vital task in the design stage. Piston as a key component of the engine that is vulnerable to severe cyclic and transient thermal and mechanical loads can be directly affected by the mentioned conversion [1, 2].

While some researchers modeled the combustion process [3], some researchers have investigated the thermoelastic stresses caused by the combustion process. Ivashchenko et al. [4] studied the stresses in a piston of a diesel engine. They employed an analytical method on the base of solving Laplace's equation to determine the von Mises equivalent stresses in specific regions of the piston, assuming a quasi-static condition. Scholz and Bargende [5] presented a three dimensional thermomechanical stress analysis of the piston, employing simultaneous computational fluid mechanics and finite element analyses. The nonlinear contact constraints have also been modeled but no experimental validation or data has been used. They calculated the velocities, accelerations, and stresses in distinct situations (crank angles of 45, 135, 225, and 315°). They reported that the maximum von Mises equivalent stress occurred at 135° crank angle at regions in contact with the gudgeon pin. Valdés et al. [6] performed velocity, acceleration, and finite element transient thermal and stress analyses for the piston, fixing some node point instead of modeling the contact constraints or using rigid links. For this reason, the stresses were unreliable in the neighborhood of the constrained nodes. They reported the equivalent stresses for the 720° of the crank shaft rotation.

Some researches were devoted to fatigue life assessment under thermo-mechanical loads. Su et al. [7] performed a thermoelastic high cycle fatigue and creep analyses in ABAQUS for the engine cylinder head and validated their stress analysis results by means of some installed strain gauges. Silva [8] analyzed thermomechanical damage fatigues in the pistons. Based on his studied on fatigue-damaged pistons, he stated that the wear, temperature gradient, and fatigue-related phenomena are the main origins of the pistons damages. He reported that the regions located at the pin holes, piston crown, grooves and skirt, are more critical. A finite element linear static analysis, using COSMOS was used for stress and temperature determination during the combustion. However, a damage analysis rather than a life assessment analysis has been performed.

In the present paper, a systematic algorithm for evaluating effects of converting a gasoline-based engine to a bifuel one on the fatigue life of the piston under the combustion thermomechanical loads. The combustion model presented previously by Jazayeri et al. [9–14], is enhanced and employed to model the combustion process for the mentioned fuels. Based on the calculated combustion pressures, temperatures and the non-uniform convection heat transfer coefficients, the combustion thermomechanical loads, the piston pin load, and the frictional and inertia forces are calculated for the gasoline and the natural gas fuels. In the stress analysis stage, higher-order Lagrangian elements are adopted to avoid stress discontinuity in the mutual boundaries of the elements. Since the available fatigue theories have been mainly proposed to check whether or not a component have infinite life, the fatigue lives are calculated by the modified Findley and McDiarmid

criteria proposed recently by Shariyat [15–18]. The fatigue lives are computed based on simulation of the standard durability tests, at the critical points of the piston. Various engineering softwares have been used to prepare the CAE and theoretical results. Finally, the temperatures, pressures, and the fatigue lives are compared with the experimental ones.

1. **Simulation of the Combustion Process**. Accurate modeling of the combustion process is a key issue for accurately comparing the engine performance in the two cases of utilizing gasoline and natural gas fuels and subsequently, for estimating the fatigue lives. In this regard, the combustion is modeled for the inline four-cylinder spark-ignited (SI) gasoline-based engine, in our computer code. The relevant engine information is listed in Table 1. Two modeling procedures are customary: (i) a closed system which models the compression and combustion stages, and (ii) an open system which covers all the stages. In the present research, the second model is used.

T a b l e 1

Specifications of the Considered Engine

Quantity	Value
Cylinder diameter	78.6 mm
Stroke	85 mm
Connecting rod length	134.5 mm
Piston eccentricity	0.8 mm
Compression ratio	11
Cylinder volume	1650 cm^3
Maximum RPM	6000
Distance between the piston pin and the C.G. of the connecting rod	40.9 mm
Engine cylinder head heat transfer area	6800 mm^2
Piston mass	0.317 kg
Connecting rod mass	0.5 kg
Inertia moment of the connecting rod	0.001738 $kg \cdot m^2$
Height of the piston	51.7 mm
Location of the piston hole relative to the top surface	29.7 mm

Information of the gasoline and the natural gas is given in Table 2. The combustion equations of the gasoline and the natural gas in the stoichiometric condition are as indicated in Eqs. (1) and (2):

$$\begin{cases} \mathrm{CNG} + x(\mathrm{O}_2 + 3.76\mathrm{N}_2) \to 1.0453\mathrm{CO}_2 + 3.9616/2\mathrm{H}_2\mathrm{O} + x \cdot 3.76\mathrm{N}_2, \\ x = 1.0453 + 3.9616/4 + 0.2 = 2.0157, \\ [AF]_{molar} = 2.0157(1 + 3.76) = 9.595, \\ [AF]_{mass} = 15.27, \end{cases} \tag{1}$$

T a b l e 2

Information of the Gasoline and the Natural Gas

Fuel type	Chemical formula	Molecular weight (kg)	Q_{LHV}, MJ/kg
Gasoline	$C_{1.0453}H_{3.961}O_{0.02}N_{0.09}$	114.82	44.00
Natural gas	$C_{8.26}H_{15.5}$	18.13	44.98

Note. Q_{LHV} is the low heating value of the reference fuels used.

$$\begin{cases} C_{8.26}H_{15.5} + 12.135(O_2 + 3.76N_2) \to 8.26CO_2 + 15.5/2H_2O + 45.6276N_2, \\ [AF]_{molar} = 12.135(1 + 3.76) = 57.76, \\ [AF]_{mass} = 14.1. \end{cases} \quad (2)$$

A two zone Vibe function is used to simulate the combustion. Crank angles corresponding to the combustion initiation and the maximum pressure are measured experimentally and given in Table 3. Since a full fatigue analysis requires the accurate and full time history of the applied thermomechanical loads, the combustion process is simulated for different rpms. The real to stoichiometric fuel ratio measured through the experiments and used in the combustion analysis is given in Table 4 for different rpms. Combustion is modeled using quasi dimensional models. In this regard, a two zone model is adopted and analyzed in our computer code. The heat release is evaluated using the same software considering a two zone Vibe model [19]. The delay in the combustion initiation is predicted based on Benson–Whitehouse model [20]. Heat transfer of the combustion chamber is investigated based on the modified Woschni's model [19]. The governing equations of the mean temperature, the mean convection heat transfer coefficient, and the rates of pressure and energy release per crank angle may be found using the first law of thermodynamics. These data are employed to perform the required heat transfer analyses. The theoretically determined temperature distributions are validated by the experimental results measured by the high temperature plugs (templugs). The procedure is somewhat similar to that explained in [9–14] but the engine information and the combustion circumstances are quite different. The resulted partial differential equations are solved employing the Runge-Kutta time integration method.

T a b l e 3

The Measured Crank Angles (deg) Corresponding to the Combustion Initiation and the Maximum Pressure at the Full Load Condition [21]

Engine rpm	Ignition advance (BTDC)		Maximum pressure angle (ATDC)	
	Gasoline	Natural gas	Gasoline	Natural gas
2000	5	23	32.0	14
3500	15	26	19.5	11
6000	14	31	21.0	8

T a b l e 4

Real to Stoichiometric Fuel Ratio for Different RPMs

Engine rpm	Natural gas	Gasoline
1250	0.962	0.895
1500	0.962	0.900
2000	0.968	0.900
2500	0.965	0.905
3000	0.970	0.900
3500	0.965	0.895
4000	0.960	0.905
4500	0.968	0.905
5000	0.970	0.875
5500	0.965	0.850
6000	0.965	0.800

2. **Kinematic**, **Dynamic**, **Force**, **Thermal**, **and Thermoelastic Stress Analyses**. Determination of the exerted forces is a vital stage for stress analysis of the components. In the present research, the forces are determined based on the prepared Matlab code based on the texts [22], our computer code and the ABAQUS CAE software, through exactly modeling the contact and large deformations nonlinearities. The employed geometric parameters are shown in Fig. 1. The frictional forces including the boundary, mixed, and hydrodynamic ones are taken into account. In contrast to the traditional calculations, effect of the distributed inertia forces is considered in the present work. Moreover, relative movement of the piston rings in their grooves is also modeled. The unknown forces have been determined based on employing the relevant force and moment equilibrium equations, taking into account D'Alembert's inertia forces and moments of the piston and the connecting rod.

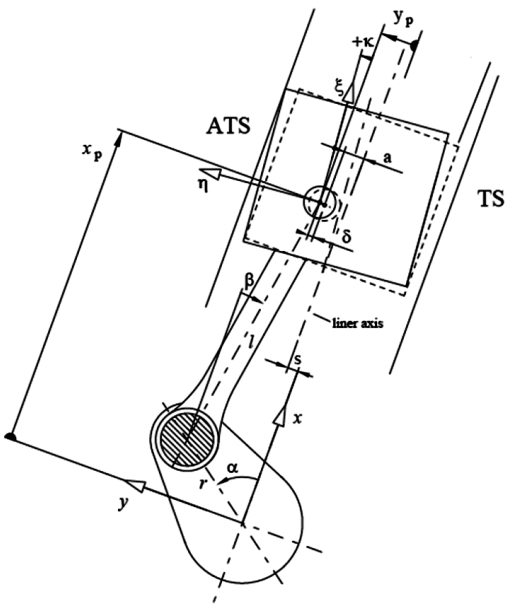

Fig. 1. Geometric parameters of the crank-piston mechanism for the kinematic and force analyses.

Based on the convection heat transfer between the piston's top surface and the combustion mixture, heat transfer between the rings and the skirt and the cylinder and subsequently, the coolant water, the heat transfer between the gudgeon pin and the coolant oil film, and the thermal loads of the piston are determined. Finally, a thermoelastic stress analysis is performed.

3. **The Fatigue Life Assessment Algorithm**. As may be expected, the resulting thermoelastic stress components vary in a non-proportional manner. Furthermore, they fluctuate with non-zero mean stresses. Therefore, the traditional fatigue life assessment criteria as well as the available critical plane high cycle fatigue (HCF) criteria may lead to unreliable results. Very comprehensive discussions have been already published by Shariyat [15–18] in this regard. Although the traditional von Mises criterion that is the base for many well-known fatigue analysis softwares, such as MSC Fatigue and FEMFAT, may lead to erroneous results in the mentioned circumstances, its results may be enhanced by employing Sine's idea of the mean stress [23] and incorporating the mean stress effect, using Goodman, Gerber, or Soderberg relations:

Goodman's linear relation:

$$\frac{\sigma_a}{\sigma_N} + \frac{\sigma_m}{\sigma_u} = 1, \tag{3}$$

Gerber's parabola:

$$\frac{\sigma_a}{\sigma_N} + \left(\frac{\sigma_m}{\sigma_u}\right)^2 = 1, \tag{4}$$

Soderberg's linear relation:

$$\frac{\sigma_a}{\sigma_N} + \frac{\sigma_m}{\sigma_Y} = 1, \tag{5}$$

where σ_a, σ_m, σ_N, σ_Y, and σ_u are the amplitude, mean stress, equivalent reversible (fatigue strength), yield, and ultimate stresses, respectively.

Among the so-called two-parameter or critical plane criteria, Fidley's and McDiarmid's criteria have been proven to be more accurate and subsequently most popular ones [24]. Findley's criterion may be expressed as [25]:

$$(\tau_a + k\sigma_n)_{\max(\theta,\,\varphi,\,\psi)} = f, \tag{6}$$

$$k = \frac{2 - \sigma_{R=-1}/\tau_{R=-1}}{2\sqrt{\sigma_{R=-1}/\tau_{R=-1} - 1}}, \qquad f = \sqrt{\frac{(\sigma_{R=-1})^2}{4(\sigma_{R=-1}/\tau_{R=-1} - 1)}}.$$

According to this criterion, the critical plane is a plane where $\max_{\theta,\,\varphi,\psi,t}(\tau_a + k\sigma_n)$ occurs. Here $\theta, \varphi,$ and ψ are the Eulerian angles and t denotes the time. Values τ_a and σ_n are the shear stress amplitude and the normal stress component, respectively, and σ_R is the fatigue strength amplitude corresponding to the specified ($R = \sigma_{\min}/\sigma_{\max}$) ratio. Based on the Goodman and Gerber mean stress correction factors, it may be expressed as:

Modified Goodman's linear equation:

$$\sigma_R = \begin{cases} \sigma_{R=-1}\left(1-\dfrac{\sigma_m}{\sigma_u}\right) & \sigma_m \geq 0, \\ \sigma_{R=-1} & \sigma_m \leq 0, \end{cases} \tag{7}$$

Gerber's equation:

$$\sigma_R = \sigma_{R=-1}\left[1-\left(\frac{\sigma_m}{\sigma_u}\right)^2\right], \tag{8}$$

where R is the ratio of the minimum to maximum stress values, and σ_R is the relevant fatigue strength amplitude. Since minus and plus mean stresses appear with similar effects in Gerber's equation, Goodman's equation is used in the present research to account for the mean stress effect.

Recently, Shariyat [15, 16] has proposed a modified Findley's criterion as

$$\tau_{eq} = \max_{\theta,\varphi,\psi,t}(\tau_a + k\sigma_n)\Big/(\sqrt{1+k^2}\,\tau_{R=-1}/\tau_R). \tag{9}$$

Modifications were proposed taking into account several parameters among them, the mean stress effect.

McDiarmid used the concept of type A and type B cracks introduced by Brown and Miller [26] to develop his linear criterion [27–29]:

$$\tau_a + k(\sigma_n)_{\max_\tau(t)} = f, \tag{10}$$

$$k = (\tau_f)_{A \text{ or } B}\big/2\sigma_u, \qquad f = (\tau_f)_{A \text{ or } B},$$

where σ_u is the ultimate strength and τ_f is the fatigue shear strength. According to this criterion, at the critical plane, $\max_{\theta,\varphi,\psi,t}(\tau_a)$ is achieved. Therefore, two limit cases (upper and lower limits) are predicted.

Recently, Shariyat [15, 16] has proposed a modified McDiarmid's criterion in the following form:

$$\tau_{eq} = [\tau_a + k(\sigma_n)_{\max_\tau(t)}]\tau_{R=-1}/\tau_R, \qquad k = \frac{2\tau_R - \sigma_R}{\sigma_m + \sigma_R}. \tag{11}$$

As the modified Findley criterion, modifications were performed taking into account several considerations (not only the mean stress effect).

The fatigue life assessment algorithm is explained in details in [16] and the related flow diagram is illustrated in Fig. 2. One of the motivations of the present research is comparing results of the modified traditional fatigue criteria that are commonly used in the engineering analysis softwares, the modified fatigue criteria of the first author, and the experimental results.

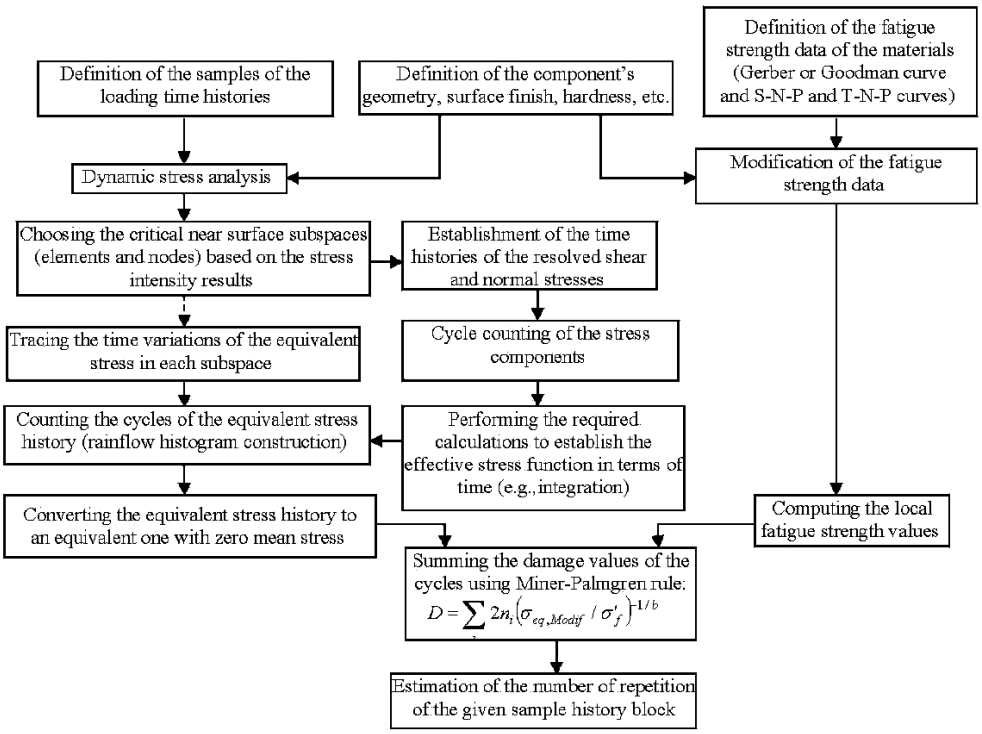

Fig. 2. Flow chart of the employed fatigue life assessment algorithm.

4. **Results**. Properties of the gasoline vary with temperature. Since temperature of the fuel varies during the 720° of the crank rotation (one combustion cycle), the following equation is used to predict the properties values at any specified temperature:

$$\overline{C}_{p\,fuel} = Af_1 + Af_2 T + Af_3 T^2 + Af_4 T^3 + Af_5 / T^2 . \tag{12}$$

The coefficients Af_1 to Af_5 are given in Table 5 [29]. While properties of the air may be determined based on the available references, variations of the combustion products may be determined based on the following equation ($\theta = T/100$) [30]:

$$\begin{cases} \overline{C}_{p\,\mathrm{N_2}} = 39.06 - 512.79\theta^{-1.5} + 1072.72\theta^{-2} - 820.4\theta^{-3}, \\ \overline{C}_{p\,\mathrm{H_2O}} = -37.57 + 30.529\theta^{0.5} - 4.1034\theta \mp 0.24198\theta^{2}, \\ \overline{C}_{p\,\mathrm{CO_2}} = 143.05 - 183.54\theta^{0.25} + 82.751\theta^{0.5} - 3.6989\theta, \\ \overline{C}_{p\,\mathrm{O_2}} = 37.432 + 0.20102\theta^{0.1.5} - 178.57\theta^{-1.5} + 236.88\theta^{-2}. \end{cases} \tag{13}$$

Property of the exhaust gases may be determined from:

$$\overline{C}_{p\,pollutant} = \frac{\overline{C}_{p\mathrm{N_2}} + \overline{C}_{p\mathrm{H_2O}} + \overline{C}_{p\,\mathrm{CO_2}} + \overline{C}_{p\mathrm{O_2}}}{8.26 + 15.5/2 + 45.6276}. \tag{14}$$

T a b l e 5

Coefficients of the Temperature-Dependency of the Material Properties of the Fuel [21]

Fuel	Weight	Af_s	Af_1	Af_2	Af_3	Af_4	Af_5	Af_6
$C_{8.26}H_{13.1}$	114.82	14.64	–24.078	256.63	–201.68	64.750	0.5808	–27.562
$C_{7.26}H_{13.1}$	106.60	14.37	–22.501	277.99	–177.26	56.048	0.4845	–17.578

Figures 3 and 4 compare the pressure of the combustion mixture versus the crank angle curves predicted by the theoretical results (results of our computer code) with those measured experimentally for the gasoline and CNG fuels, for 3500 rpm (corresponding to the maximum torque) and 6000 rpm (corresponding to the maximum power), respectively. The theoretical results are in a good agreement with the experimental results. Furthermore, comparing results appeared in Figs. 3 and 4 reveal that replacing the gasoline with the natural gas may lead to a slight change in the resulted pressure profile in the 3500 rpm, the difference will be significant in the 6000 rpm. Therefore, the engine acceleration will be affected remarkably.

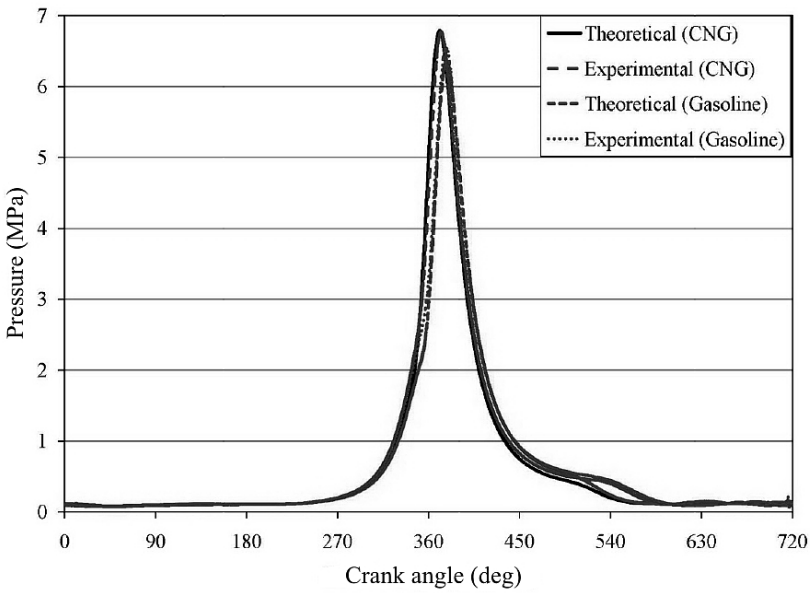

Fig. 3. In-cylinder pressure variations versus crank angle for a set of theoretical and experimental results using gasoline and natural gas at 3500 rpm.

Figures 5 and 6 illustrate variations of the computed temperature of the combustion mixture and the coefficient of the heat convection of the top surface of the piston, with the crank angle at 6000 rpm, respectively. Since the temperature distributions are somewhat identical, due to higher coefficient of the convection heat transfer, it seems that the thermal losses may be higher for the CNG fuel.

Figures 7 and 8 illustrate the vertical and horizontal components of the resultant forces exerted on the piston, respectively for the gasoline and CNG fuels at 3500 and 6000 rpm. As it may be noted from Figs. 7 and 8, the maximum forces are exerted slightly after the combustion initiation. Furthermore, the vertical

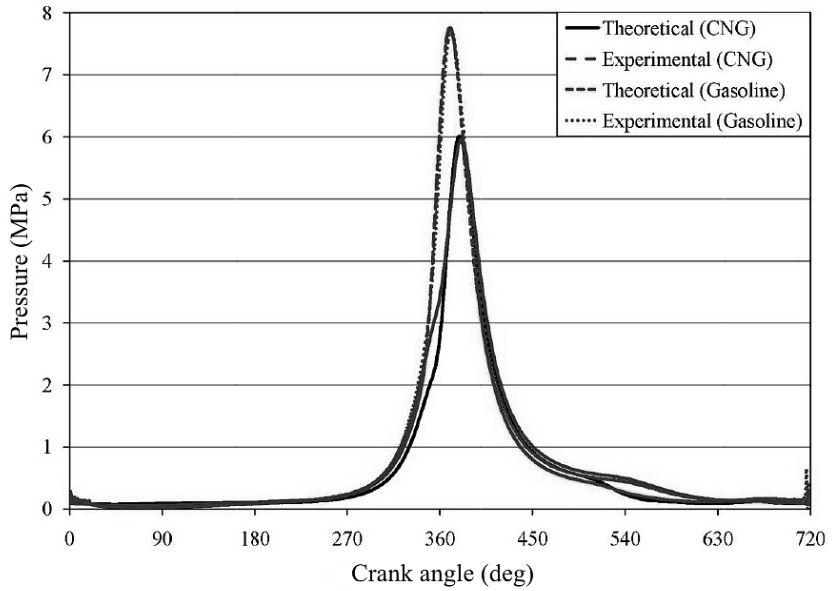

Fig. 4. In-cylinder pressure variations versus crank angle for a set of theoretical and experimental results using gasoline and natural gas at 6000 rpm.

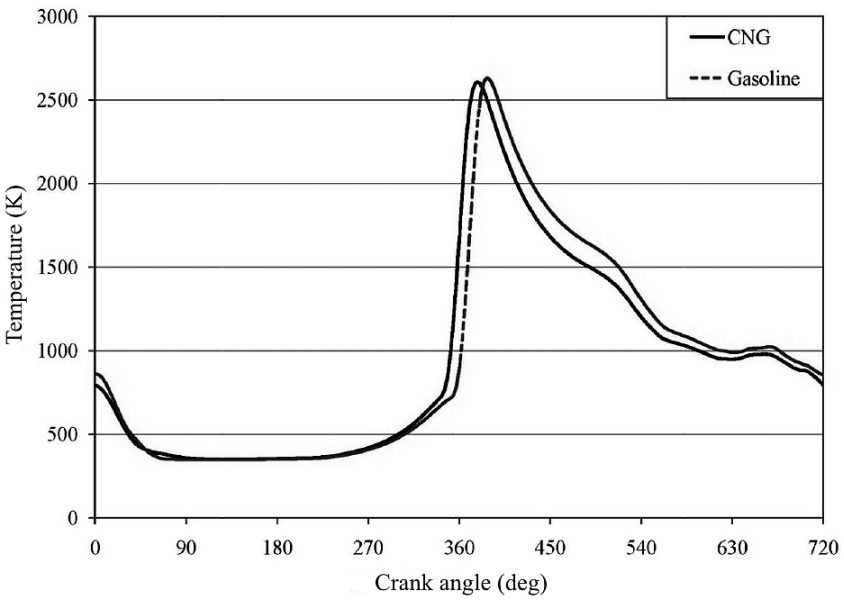

Fig. 5. Comparison of the mixture temperature for the gasoline and CNG fuels at 6000 rpm.

component is the dominant one. Variations of the translational acceleration of piston are depicted in Fig. 9, for the gasoline fuel. Variations of the frictional force are shown in Fig. 10 for the thrust side of the piston's skirt, at 3500 and 6000 rpm for the gasoline and CNG fuels. As it may be readily seen, the frictional forces at the top dead centre (TDC) and bottom dead center (BDC) are of a boundary nature [31] and are subsequently, high whereas at the midway point, the friction is of a hydrodynamic nature and leads to small frictional forces.

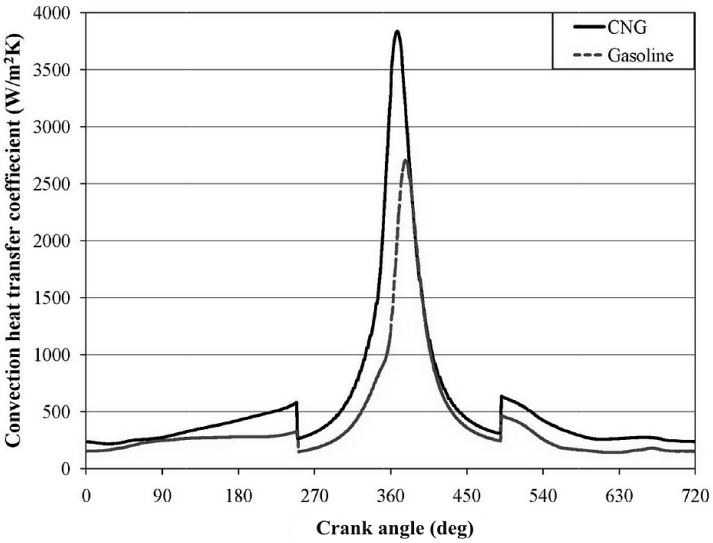

Fig. 6. Comparison of the coefficients of the convection heat transfer for the gasoline and CNG fuels at 6000 rpm.

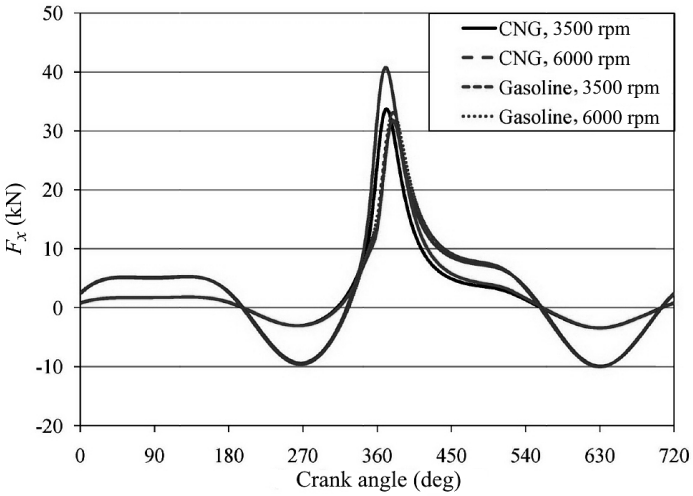

Fig. 7. A comparison among the vertical component of the resultant force exerted on the piston at 3500 and 6000 rpm for the gasoline and CNG fuels.

The finite element analysis (FEA) model of the piston has been constructed in Hypermesh software. Optimized second-order Lagrangian elements are adopted to avoid abrupt jumps in the stress components at the mutual boundaries of the elements. The FEA model is validated through a modal analysis in the NASTRAN/PATRAN software. The proper size of the element is chosen based on a convergence analysis. After accurately defining of the contact regions (between the piston and the cylinder and between the piston hole and the gudgeon pin) and constraints, the inertial, frictional, and the thermomechanical combustion loads obtained in the foregoing steps are imposed. The inertia relief method is employed. In the contact region of the rings, skirt, and pin of the piston, the mean temperature of the lubricant film and the proper coefficients of the convection heat transfer are used.

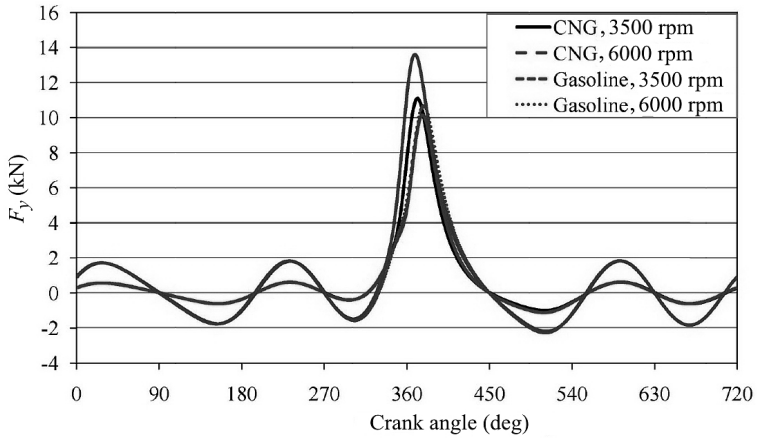

Fig. 8. A comparison among the horizontal component of the resultant force exerted on the piston at 3500 and 6000 rpm, for the gasoline and CNG fuels.

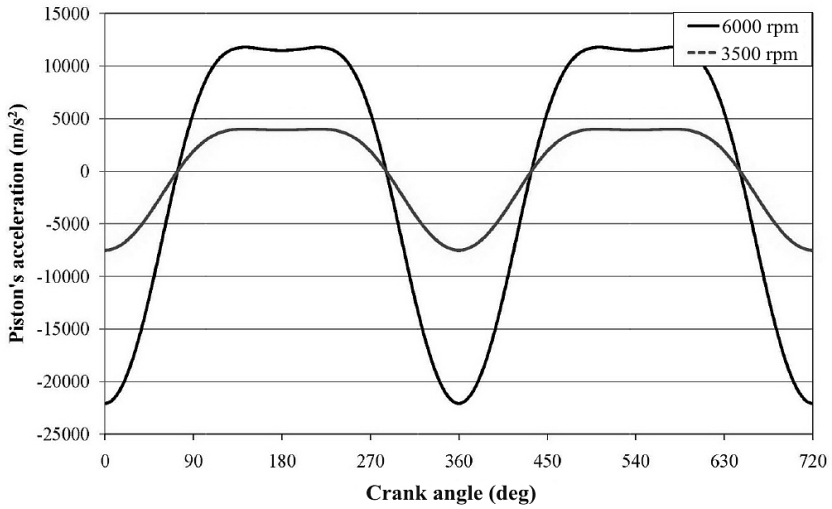

Fig. 9. Variations of the translational acceleration at 3500 and 6000 rpm.

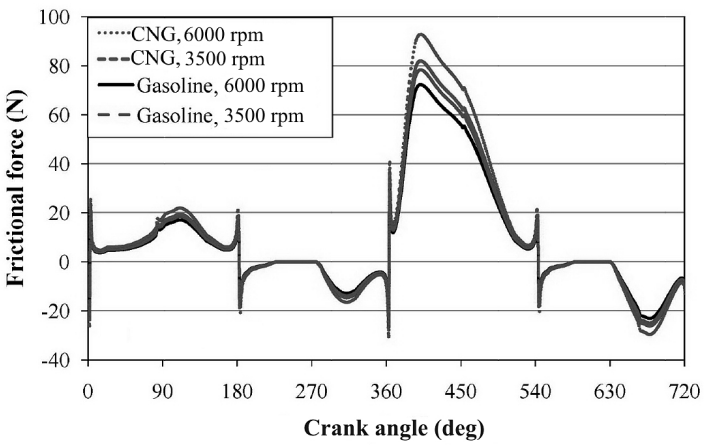

Fig. 10. Variations of the frictional force for the thrust side of the piston's skirt at 3500 and 6000 rpm for gasoline and CNG fuels.

Figure 11 illustrates the temperature distribution of the piston at 6000 rpm for both gasoline and CNG fuels, as a typical result. The temperature distribution has been validated experimentally by means of TEMPLUGs shown in Fig. 12. The relevant von Mises equivalent stresses are shown in Fig. 13, for the most critical situation (370° of the crank angle) at 6000 rpm for the CNG fuel, as representative results. The maximum calculated temperature is 252℃ which shows a good agreement with the result measured by the templugs (249℃).

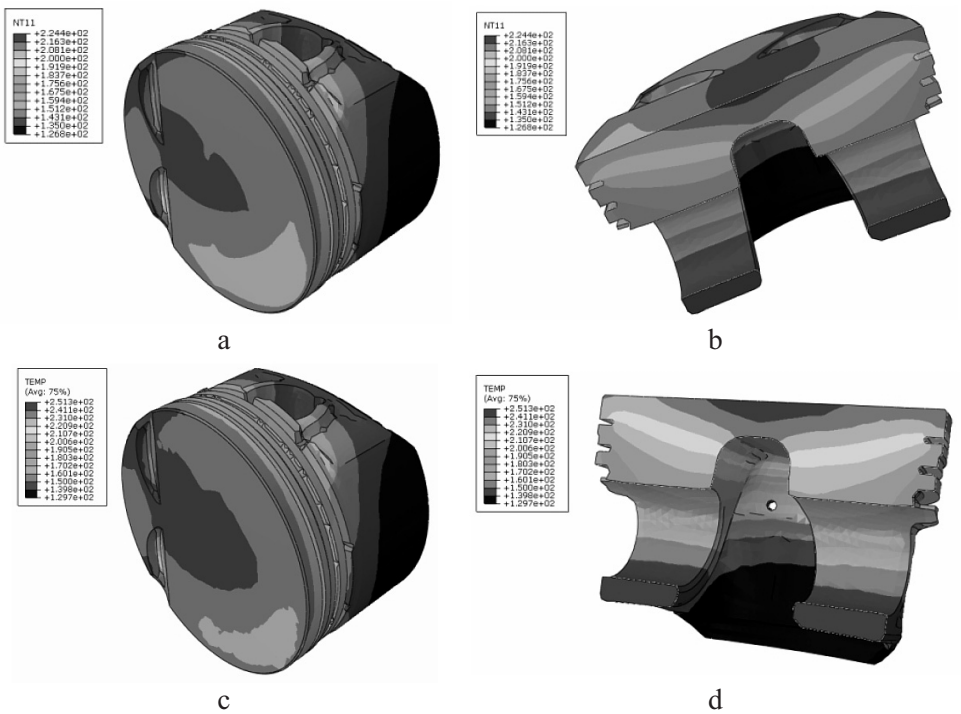

Fig. 11. Temperature distribution in 6000 rpm for the (a, b) gasoline and (c, d) CNG fuels.

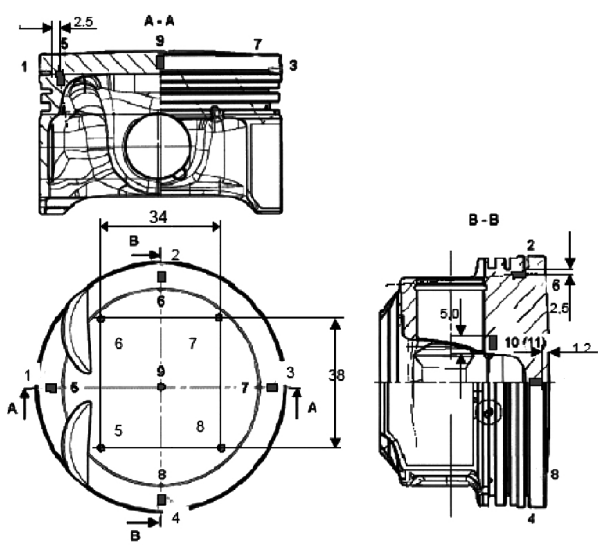

Fig. 12. The temperature plugs used to validate the computed temperatures.

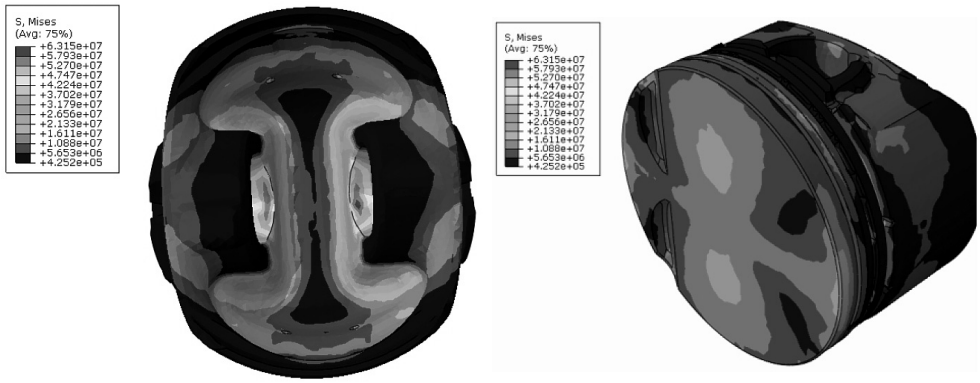

a

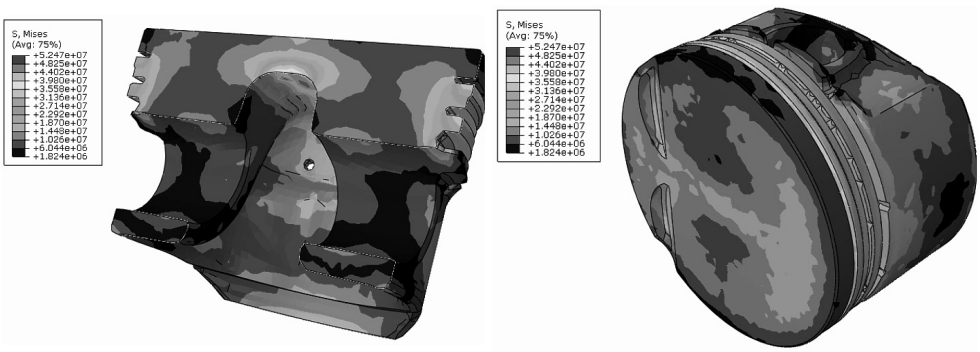

b

Fig. 13. Distribution of the: (a) mechanical and (b) thermal von Mises stresses at 6000 rpm and 370° crank angle, for the CNG fuel.

Fig. 14. Orientations of the most critical regions.

Results shown in Fig. 13 reveal that the stresses are more critical in the neighborhood of node No. 707 of Fig. 14. Regions located in the neighborhood of node No. 7200 experiences the maximum pure thermal von Mises stress. Although regions with greatest von Mises equivalent stress may not be generally considered as regions with worst fatigue lives, fatigue results obtained by the MSC Fatigue

software have also confirmed that for the considered conditions, regions located around node points Nos. 707 and 7200 are most critical. Time variations of the equivalent stresses of the piston are mainly due to variations of the mechanical stresses. Variations of the von Mises equivalent mechanical stress of nodes Nos. 707 and 7200 are depicted in Figs. 15 and 16 for a complete combustion cycle of the gasoline as well as CNG fuels, for 3500 and 6000 rpm. From these figures, it may be deduced the maximum and minimum stresses occurs at crank angles of 370 and 1°, respectively. For this reason, regions in the neighborhood of node No. 707 are adopted as critical ones.

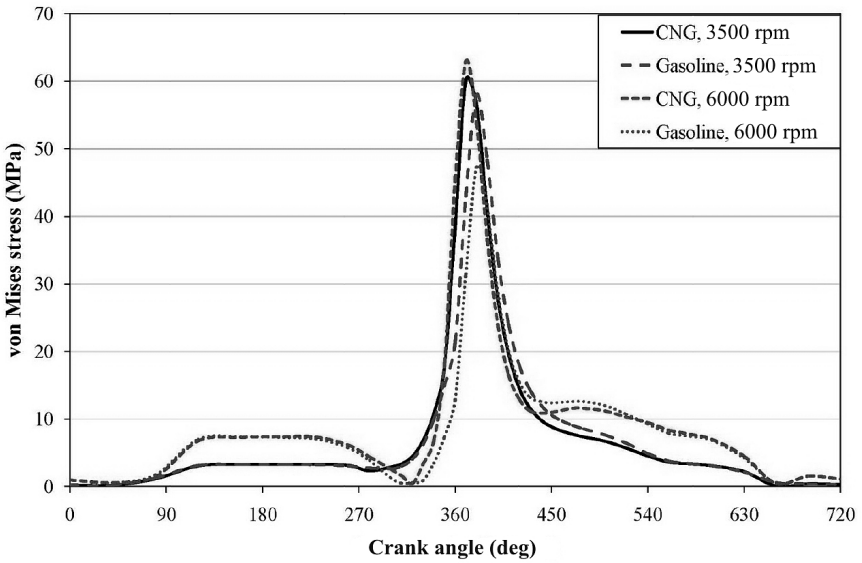

Fig. 15. Variations of the von Mises equivalent mechanical stress of node No. 707 for the complete combustion cycle of the gasoline as well as CNG fuels at 3500 and 6000 rpm.

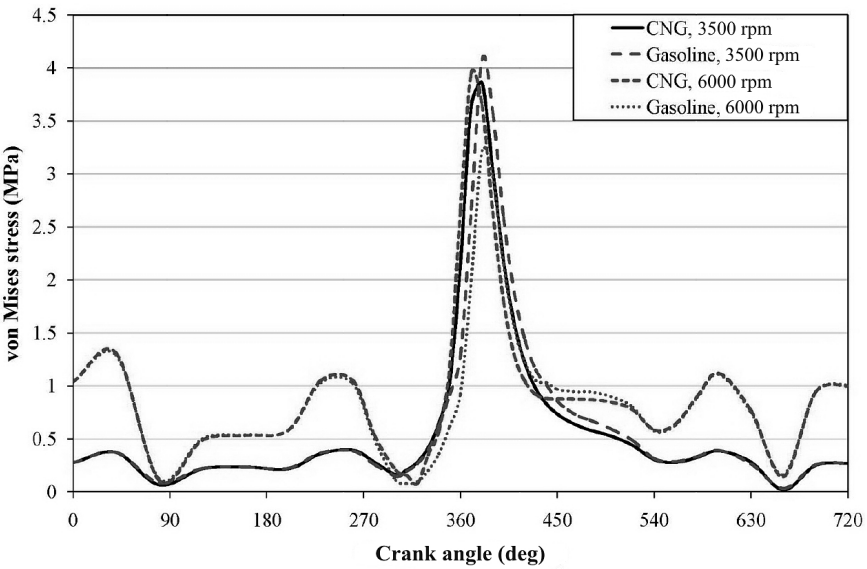

Fig. 16. Variations of the von Mises equivalent mechanical stress of node No. 7200 for the complete combustion cycle of the gasoline as well as CNG fuels at 3500 and 6000 rpm.

As it has been mentioned in Section 3, in the present research, the fatigue life results are extracted based on the modified von Mises, modified version of the Findley and McDiarmid theories proposed by Shariyat, and the experimental methods. The employed fatigue life assessment algorithm has not been proposed by any other authors before. The equivalent Findley and McDiarmid stresses (Eqs. 9 and 11) are computed at the critical points of the piston and the relevant fatigue lives have been calculated based on computer codes written by the authors, for the 720° of the crank rotation. Some fatigue damages predicted by different approaches, various engine rpm and fuel types are shown in Table 6 for regions surrounding nodes Nos. 707 and 7200, as typical results. As it may be noted from results of Table 6, node No. 707 is the most critical node.

T a b l e 6

Fatigue Damages Predicted by Different Approaches for Regions Surrounding Nodes Nos. 707 and 7200 for Various RPMs

Fatigue life assessment approach	No. node	750 rpm	3500 rpm	6000 rpm
von Mises (Goodman mean stress correction)	707	$\frac{1.0018\cdot10^{-13}}{4.8383\cdot10^{-13}}$	$\frac{2.1316\cdot10^{-10}}{5.8102\cdot10^{-10}}$	$\frac{1.6211\cdot10^{-11}}{3.5025\cdot10^{-9}}$
	7200	$\frac{1.0602\cdot10^{-17}}{1.1319\cdot10^{-16}}$	$\frac{6.7149\cdot10^{-13}}{6.3760\cdot10^{-12}}$	$\frac{1.0102\cdot10^{-13}}{2.8745\cdot10^{-11}}$
von Mises (Gerber mean stress correction)	707	$\frac{4.3994\cdot10^{-14}}{2.6188\cdot10^{-13}}$	$\frac{6.3924\cdot10^{-11}}{1.6768\cdot10^{-10}}$	$\frac{5.6012\cdot10^{-12}}{1.9938\cdot10^{-9}}$
	7200	$\frac{9.2547\cdot10^{-18}}{1.0597\cdot10^{-17}}$	$\frac{3.5331\cdot10^{-13}}{3.3628\cdot10^{-12}}$	$\frac{5.7755\cdot10^{-14}}{1.2537\cdot10^{-11}}$
von Mises (Soderberg mean stress correction)	707	$\frac{1.8844\cdot10^{-13}}{4.9675\cdot10^{-12}}$	$\frac{7.2651\cdot10^{-10}}{2.1891\cdot10^{-9}}$	$\frac{4.1897\cdot10^{-11}}{9.3645\cdot10^{-9}}$
	7200	$\frac{1.3290\cdot10^{-17}}{1.5282\cdot10^{-16}}$	$\frac{1.0548\cdot10^{-12}}{9.9942\cdot10^{-12}}$	$\frac{1.4765\cdot10^{-13}}{5.4480\cdot10^{-11}}$
Modified Findley	707	$\frac{1.4897\cdot10^{-14}}{6.0455\cdot10^{-14}}$	$\frac{7.4480\cdot10^{-12}}{7.9051\cdot10^{-12}}$	$\frac{9.0612\cdot10^{-13}}{8.1219\cdot10^{-11}}$
	720	$\frac{2.2317\cdot10^{-19}}{3.6071\cdot10^{-17}}$	$\frac{1.1870\cdot10^{-14}}{7.2067\cdot10^{-14}}$	$\frac{3.3429\cdot10^{-15}}{1.3436\cdot10^{-12}}$
Modified McDiarmid	707	$\frac{7.0654\cdot10^{-15}}{1.2416\cdot10^{-13}}$	$\frac{2.5676\cdot10^{-12}}{5.9044\cdot10^{-11}}$	$\frac{3.1148\cdot10^{-13}}{1.8382\cdot10^{-10}}$
	7200	$\frac{6.3715\cdot10^{-18}}{9.3908\cdot10^{-16}}$	$\frac{1.8248\cdot10^{-13}}{1.4798\cdot10^{-14}}$	$\frac{1.5411\cdot10^{-16}}{1.0742\cdot10^{-12}}$
FEMFAT software	707	$\frac{6.74\cdot10^{-14}}{2.80\cdot10^{-14}}$	$\frac{6.90\cdot10^{-12}}{7.22\cdot10^{-11}}$	$\frac{9.31\cdot10^{-13}}{1.10\cdot10^{-10}}$
	7200	$\frac{5.80\cdot10^{-19}}{1.20\cdot10^{-18}}$	$\frac{2.14\cdot10^{-16}}{7.80\cdot10^{-16}}$	$\frac{1.81\cdot10^{-18}}{6.00\cdot10^{-14}}$

Note. Here and in Table 9: the data cited over the line correspond to gasoline and under the line – to CNG.

As a second stage, two standard histograms are adopted to simulate the service thermomechanical loads and extract the fatigue results. The corresponding block programs are given in Tables 7 and 8. The corresponding fatigue test conditions are also specified in the mentioned tables. The first standard block program is corresponding to the so-called 800 h durability under mechanical loads test whereas the second one is associated with the so-called 400 h durability under thermal loads test.

Table 7

Block Program of the 800 h Mechanical Engine Durability Test

Event order	Duration (min)	Engine speed (rpm)	Load spec.	Outlet coolant water temperature (°C)	Maximum oil temperature (°C)
1	5	6000	rated power	90^{+3}	140
2	4	2000	BMEP = 2 bar		
3	5	3500	max torque		
4	1	750	low idle		

Table 8

Block Program of the 400 h Thermal Engine Durability Test

Event order	Duration (min)	Engine speed (rpm)	Load spec.	Outlet coolant water temperature (°C)
1	9.5	6000	rated power	90^{+3}
2	4.5	750	low idle	30^{+10}

As it has been mentioned before, the most critical regions of the piston are the pin hole, piston's crown, and piston's skirt (at the thrust side) (precisely, regions located in the neighborhood of node points Nos. 707 and 7200). The reliability contours obtained by FEMFAT software and illustrated in Fig. 17, confirm this conclusion.

Table 9 summarizes the normalized fatigue results. The results are normalized by dividing them by the experimental results. It is known that in non-proportional loadings, von Mises criterion usually leads to results that are extremely conservative [23]. In the present analysis, von Mises criterion is modified using Goodman, Gerber, and Soderberg mean stress corrections. Although modified von Mises criterion has been employed in the present research, the relevant results show significant errors. Results of Table 9 reveal that employing Gerber and Soderberg mean stress corrections leads to most and least accurate results for the von Mises-type criteria. Furthermore, results of Table 9 reveal that modified McDiarmid and Findley criteria lead to more accurate results with the modified Findley criterion regenerates the experimental results more accurately. Moreover, an interesting conclusion may be deduced from results of Table 9: although absolute life values predicted by various theories show remarkable discrepancies, the comparative results (e.g., the relative lives of the CNG and gasoline engines), may

T a b l e 9

Normalized Fatigue Lives (by Dividing the Original Results to the Experimental Ones), Predicted Based on Various Theories for the So-Called 800 h Durability Tests

Approach	Normalized fatigue damage	Normalized fatigue life	Normalized gasoline to CNG engines
von Mises (Goodman's mean stress correction)	30.9 / 31.8	29.048 / 23.568	16.40
von Mises (Gerber's mean stress correction)	9.26 / 18.10	8.730 / 12.630	31.20
von Mises (Soderberg's mean stress correction)	105.0 / 85.1	96.825 / 91.457	12.90
Modified Findley	1.080 / 0.738	1.064 / 0.519	10.90
Modified McDiarmid	0.372 / 1.670	0.365 / 1.685	7.16
Experimental	1.0 / 1.0	1.0 / 1.0	15.90

T a b l e 1 0

Ratio of the Fatigue Lives Predicted Based on Various Theories (400 to 800 h Test Results)

Approach	Ratio of the fatigue lives (400 to 800 h test results)
von Mises (Goodman's mean stress correction)	0.892473
von Mises (Gerber's mean stress correction)	0.840246
von Mises (Soderberg's mean stress correction)	0.888942
Modified Findley	0.84
Modified McDiarmid	1.022222
Experimental	1.208955

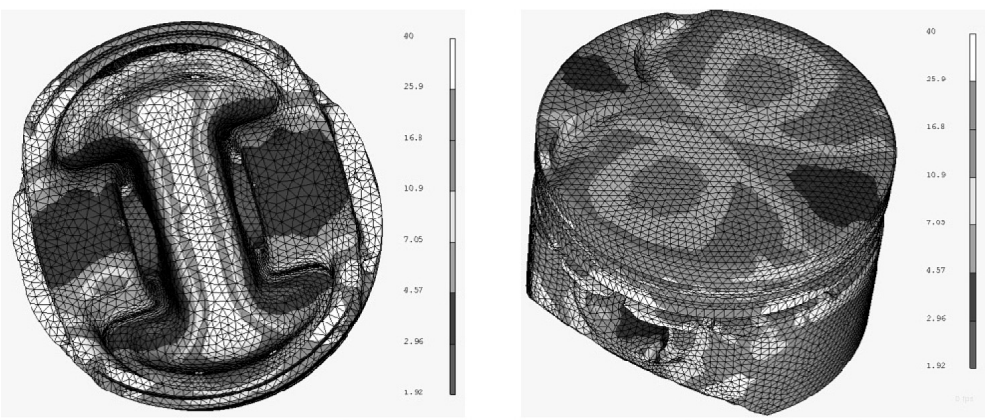

Fig. 17. Reliability contours of the piston derived by the FEMFAT software for the CNG fuel (6000 rpm).

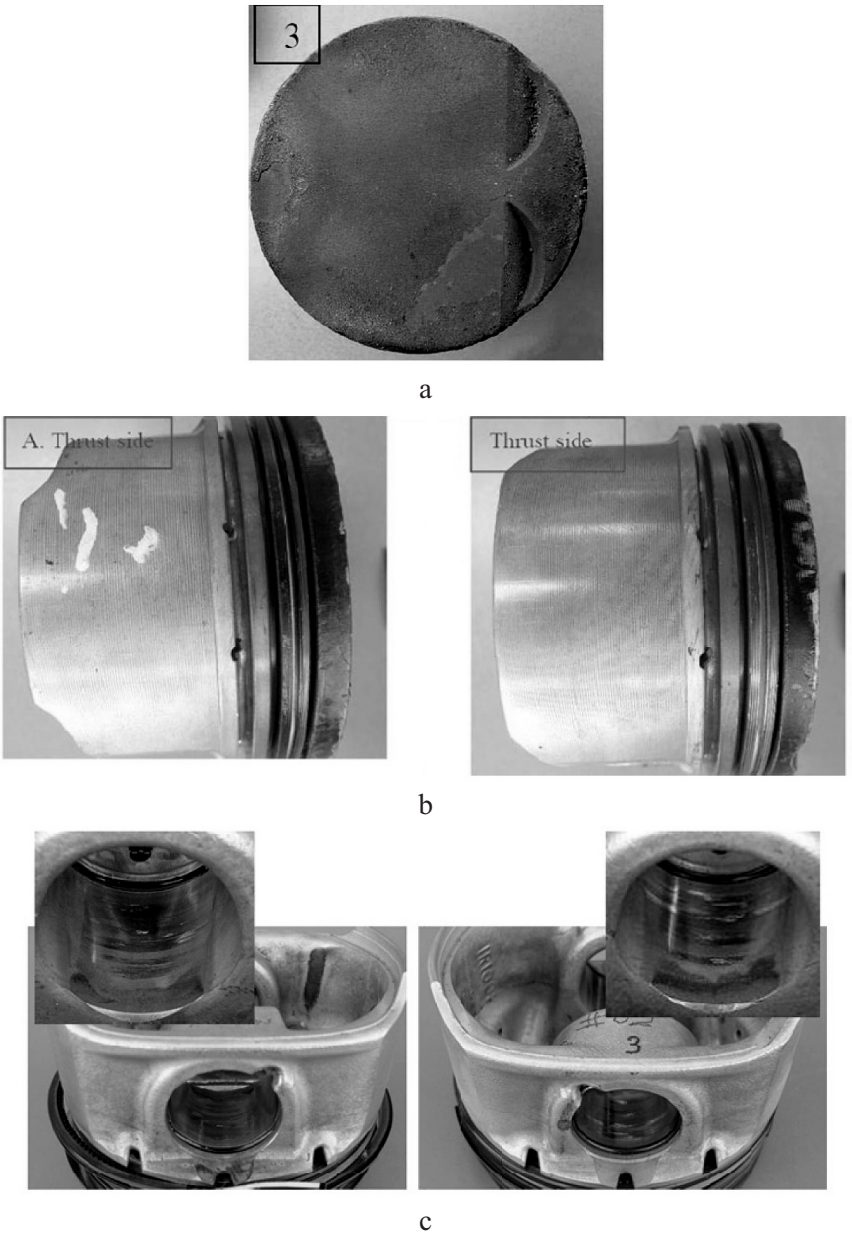

Fig. 18. Some of the observed piston's defects during the fatigue tests: (a) destruction of the piston crown in the so-called 800 h durability test, (b) destruction of the piston trust side of the skirt in the so-called 800 h durability test, and (c) destruction in the piston's pin hole in a so-called 400 h durability test.

show acceptable deviations from the experimental comparative results. It is evident that the experimental results have been calculated based on mean values of results obtained from numerous fatigue tests with identical conditions. Ratio of the fatigue lives of the two types of the durability tests predicted based on various theories (400 to 800 h test results) are given in Table 10. As it may be seen, results of the modified McDiarmid criterion are closer to the experimental ratio.

Fatigue failures have been detected based on visual NDT techniques, e.g., spot check for micro-crack detection. Some of the defects occurred for the piston through the fatigue tests are shown in Fig. 18.

Conclusions. In the present research, a systematic performance and fatigue analysis procedure is presented for the pistons with an emphasis on employing and validating the three-dimensional multiaxial random fatigue criteria recently proposed by the first author. These analyses are vital, e.g., when upgrading a gasoline-based engine to a CNG engine. In this regard, results of the enhanced traditional theories and the recently proposed theories have been compared with the experimental results for a part with complicated geometry, boundary conditions, and loading conditions. The customary method of verifying the results by means of simple specimens, and simple boundary and loading conditions may not guarantee validation of the results in more complex conditions. The obtained results for the combustion temperatures and pressures, the temperature distributions, and the fatigue life results obtained by the recently proposed critical plane-type criteria of the first author, have a good agreement with the experimental results.

Acknowledgments. The authors would like to thank IPCO Engine Research Company for its cooperation in extracting the experimental data.

Р е з ю м е

Представлено систематизовану методику теоретичної оцінки робочих характеристик газового двигуна внутрішнього згоряння і параметрів утомного руйнування його поршнів та виконано її експериментальну верифікацію шляхом натурних випробувань двигуна. Методика включає моделювання процесів внутрішнього згоряння і теплопередачі, кінематичний і динамічний аналізи рухомих частин двигуна, аналіз перехідного термопружного процесу й утомного руйнування при комплексному термомеханічному навантаженні. Розрахункові значення тиску і температури для різних кутів повороту кривошипно-шатунного механізму добре узгоджуються з експериментальними даними. Результати розрахунку характеристик теплопередачі підтверджуються даними експериментальних вимірювань за допомогою термодатчиків Templugs. Рухома система вважається не дискретною, а неперервною з точно модельованими нелінійними багатоточковими контактними реакціями. При розрахунках утомної довговічності використовуються модифіковані критерії Мак-Діарміда і Фіндлі для багатоциклової утоми, запропоновані одним з авторів работи. Виконано їх верифікацію за допомогою експериментальних даних. Методику можна використовувати для оцінки доцільності перетворення бензинового двигуна в газовий. Розрахункові дані щодо різних утомних характеристик, отримані в умовах термомеханічного навантаження, підтверджують точність запропонованих критеріїв утоми і показують, що термін служби поршня двигуна внутрішнього згоряння суттєво зменшується, якщо замість бензину використовувати природний газ.

1. M. Shariyat and P. Djamshidi, “Minimizing the engine-induced harshness based on the DOE method and sensitivity analysis of the full vehicle NVH model,” *Int. J. Automotive Tech*., **10**, 687–696 (2009).

2. S. J. Kim, S. G. Kim, K. S. Oh, and S. K. Lee, "Excitation force analysis of a power train based on CAE technology," *Int. J. Automotive Tech*., **9** (6), 703–711 (2008).

3. H. Kajiwara, Y. Fujioka, T. Suzuki, and H. Negishi, "An analytical approach for prediction of piston temperature distribution in diesel engines," *JSAE Rev.*, **23**, 429–34 (2002).

4. N. A. Ivashchenko, R. A. Nasyrov, and A. V. Timokhin, "Evaluationof the thermal and stress-strain state of an internal combustion engine piston by the finite-element method," *Strength Mater*., **12**, No. 2, 187–192 (1980).

5. B. Scholz and M. Bargende, *Three-Dimensional Simulation of the Piston Group*, SAE Technical Paper No. 2000-01-1239 (2000).

6. M. Valdés, J. Casanova, A. Rovira, and M. Trinidad, *Design of Carbon Pistons Using Transient Heat Transfer and Stress Analyses*, SAE Technical Paper 2001-01-3217 (2001).

7. X. Su, M. Zubeck, J. Lasecki, et al., *Thermal Fatigue Analysis of Cast Aluminum Cylinder Heads*, SAE Technical Paper No. 2002-01-0657 (2002).

8. F. S. Silva, "Fatigue on engine pistons – A compendium of case studies," *Eng. Failure Anal.*, **13**, 480–492 (2006).

9. S. A. Jazayeri, M. Sharifi Rad, and S. Azadi, "Development and validation for mean value engine models," in: ASME Tech. Conf., Int. Combus. Eng. Div., Paper No. ICEF2005-1267 (2005), pp. 19–28.

10. S. A. Ghazi Mir Saied, S. A. Jazayeri, and A. H. Shamekhi, "Modeling of variable intake valve timing in SI engine," in: ASME Tech. Conf., Int. Combus. Eng. Div., Paper No. ICES2006-1411 (2006), pp. 789–803.

11. S. N. Shahangian, S. A. Jazayeri, and N. Bagheri, "Study on characteristics of HCCI engine operation for EGR, equivalence ratio and intake charge temperature and pressure while using dimethyl ether," in: ASME Tech. Conf., Int. Combus. Eng. Div., Paper No. ICEF2007-1644 (2007), pp. 127–137.

12. A. Mohammadi, S. A. Jazayeri, and M. Ziabasharhagh, "Numerical simulation of convective heat transfer in a spark ignition engine," in: ASME Tech. Conf., Int. Combus. Eng. Div., Paper No. ICES2008-1687 (2008).

13. S. N. Shahanigan, M. Keshavarz, G. Javadirad, et al., "A theoretical study on performance and combustion characteristics of HCCI engine operation with diesel surrogate fuels: n-heptane, dimethyl ether," in: ASME Tech. Conf., Int. Combus. Eng. Div., Paper No. ICES2008-1682 (2008).

14. O. Jahanian and S. A. Jazayeri, "A comprehensive study on natural gas HCCI engine response to different initial conditions via a thermo-kinetic engine model," in: ASME Tech. Conf., Int. Combus. Eng. Div., Paper No. ICEF2009-14084 (2009).

15. M. Shariyat, "A fatigue model developed by modification of Gough's theory, for random non-proportional loading conditions and three-dimensional stress fields," *Int. J. Fatigue*, **30**, 1248–1258 (2008).

16. M. Shariyat, "Two new multiaxial HCF criteria based on virtual stress amplitude and virtual mean stress concepts, for complicated geometries and random non-proportional loading conditions," *Trans. ASME*, *J. Eng. Mater. Technol.*, **131**, No. 3, 031014, 1–13 (2009).
17. M. Shariyat, "Three energy-based multiaxial HCF criteria for fatigue life determination in components under random non-proportional stress fields," *Fatigue Fract. Eng. Mater. Struct.*, **32**, 785–808 (2009).
18. M. Shariyat, "New HCF theories based on the instantaneous damage tracing in components with complicated geometries and three dimensional random non-proportional stress fields," *Int. J. Damage Mech*., **19**, 659–690 (2010).
19. P. S. Ferfuson and A. T. Kirkpatrick, *Internal Combustion Engines Applied Thermosciences*, John Wiley & Sons Inc. (2000).
20. J. Ramos, *Internal Combustion Engines*, McGraw-Hill (1992).
21. J. B. Heywood, *Internal Combustion Engine Fundamentals*, McGraw-Hill (1988).
22. A. Erdman, G. N. Sandor, and S. Kota, *Mechanism Design: Analysis and Synthesis*, Prentice Hall (2000).
23. D. F. Socie and G. B. Marquis, *Multiaxial Fatigue*, SAE International (2000).
24. A. Bernasconi, S. Foletti, and I. V. Padopoulos, "A study on combined torsion and axial load fatigue limit tests with stresses of different frequencies," *Int. J. Fatigue*, **30**, 1430–1440 (2008).
25. W. N. Findley, "A theory for effect of mean stress on fatigue of metals under combined torsion and axial load or bending," *Trans. ASME*, *J. Eng. Ind*., **81**, 301–306 (1959).
26. M. W. Brown and K. J. Miller, "A theory for fatigue failure under multiaxial stress-strain conditions," *Proc. Inst. Mech. Eng*., **187**, 745–755 (1973).
27. D. L. McDiarmid, "Fatigue under out-of-phase bending and torsion," *Fatigue Fract. Eng. Mater. Struct.*, **9**, 457–475 (1987).
28. D. L. McDiarmid, "A general criterion for high cycle multiaxial fatigue failure," *Fatigue Fract. Eng. Mater. Struct.*, **14**, 429–453 (1991).
29. D. L. McDiarmid, "A shear stress based critical-plane criterion of multiaxial fatigue failure for design and life prediction," *Fatigue Fract. Eng. Mater. Struct.*, **17**, 1475–1484 (1994).
30. R. E. Sonntag, C. Borgnakke, and G. J. Van Wylen, *Fundamentals of Thermodynamics*, 6th edition, John Wiely & Sons Inc. (2002).
31. S. C. Tung and M. L. McMillan, "Automotive tribology overview of current advances and challenges for the future," *Trib. Int*., **37**, 517–536 (2004).

Received 11. 05. 2011